Micro pump Formation Induced by catalytic Hydrolysis of Phosphodiester Bond

Anuj Kaundal

MS16081

A dissertation submitted for the partial fulfilment of

BS-MS dual degree in Science

Department of Chemical Sciences

Indian Institute of Science Education and Research Mohali

April 2021

Certificate of Examination

This is to certify that the dissertation titled **"**Micro pump Formation Induced by catalytic Hydrolysis of Phosphodiester Bond**"** submitted by Mr. Anuj Kaundal (Reg. No. MS16081) for the partial fulfilment of BS-MS dual degree programme of the Institute has been examined by the thesis committee duly appointed by the Institute. The committee finds the work done by the candidate satisfactory and recommends that the report be accepted.

Dr.Santanu Kumar Pal	Dr. Sabyasachi Rakshit	Dr.Subhabrata Maiti
		(Supervisor)
Assoc. Professor	*Assoc. Professor*	*Asst. Professor*
IISER Mohali	*IISER Mohali*	*IISER Mohali*

Dated: 30th April 2021

Declaration

The work presented in this dissertation has been carried out by me under the guidance of Dr. Subhabrata Maiti at the Department of Chemical Sciences, Indian Institute of Science Education and Research Mohali.

This work has not been submitted in part or in full for a degree, a diploma, or a fellowship to any other university or institute. Whenever contributions of others are involved, every effort is made to indicate this clearly, with due acknowledgement of collaborative research and discussions. This thesis is a bonafide record of original work done by me and all sources listed within have been detailed in the bibliography.

Anuj kaundal

(Candidate)

Dated: 30th April 2021

In my capacity as the supervisor of the candidate's project work, I certify that the above statements by the candidate are true to the best of my knowledge.

Dr. Subhabrata Maiti

(Supervisor)

Acknowledgement

First and foremost, I would like to express my sincere gratitude to my thesis supervisor Dr. Subhabrata Maiti for the continuous support throughout the period of my MS-thesis project, for his patience, enthusiasm, and immense knowledge. On many occasions, he had given me valuable suggestions that directed me towards the right path and motivated me to learn new entities. I would also like to thank my committee members Dr. Sabyasachi Rakshit and Dr. Santanu Kumar Pal for providing me an opportunity to present my work and for their invaluable discussions and suggestions. Furthermore, I would like to express my heartful thanks to Ms. Priyanka, with whom I worked on this project, for her valuable advice and discussions and consistent help throughout my project. I would also like to thank my other lab members Ms. Akshi Deshwal, Ms. Ekta Shandilya and Mr. Rishi Ram Mahato, for their valuable advice and help at various steps of my project and to maintain a knowledgeable and peaceful environment in the lab.

Last but most significant, it gives me immense pleasure to express my gratitude to my beloved parents Mr. Piar Chand and Mrs. Kusum lata who have always believed in me and supported me with unconditional love throughout my life. I would also like to express my gratitude to my friends, siblings for their immense support.

List of Figures

List of schemes

List of Abbreviations

HPNPP	2-hydroxypropyl-*p*-nitrophenyl phosphate
BPNPP	bis(p-nitrophenyl)phosphate
PNPP	p-nitrophenyl picolinate
PNP	p-nitrophenolate
BAPA	bis-(2-amino-pyridinyl-6-methyl)amine
TACN	1, 4, 7-triazacyclononane
TACN-DiBoc	Di-tert-butyl 1, 4, 7-triazacyclononane-1, 4-dicarboxylate
$C_{16}H_{33}Br$	1-bromohexadecane
C_{16}TACN-DiBoc	Di-tert-butyl 7-hexadecyl-1, 4, 7-triazacyclononane-1, 4-dicarboxylate
C_{16}TACN	1-hexadecyl-1, 4, 7-triazacyclononane
DBU	1, 8-Diazabicyclo [5, 4, 0] undec-7-ene
Boc_2O	Di-tert-butyl dicarbonate
$CHCl_3$	Chloroform
DCM	Dichloromethane

MeOH	Methanol
MeCN	Acetonitrile
S-9-Br	S-(9-bromononyl) ethanethioate
S-9 –TACN-DiBoc	Di-tert-butyl 7-(9-(acetylthio) nonyl)-1, 4, 7-triazacyclononane-1, 4- dicarboxylate
TACN-SH	9-(1, 4, 7-triazacyclononan-1-yl) nonane-1-thiol
DPA	Dipicolylamine
S-9-DPASOCH$_3$	S-(9-(bis (pyridin-2-ylmethyl) amino) nonyl) ethanethioate
DPA-SH	9-(bis (pyridin-2-ylmethyl) amino) nonane-1-thiol
NaOH	Sodium Hydroxide
HCl	Hydrochloric acid
$C_{12}H_{25}Br$	1-bromododecane
C_{12}TACN-DiBoc	di-tert-butyl 7-dodecyl-1,4,7-triazacyclononane-1,4-dicarboxylate
C_{12}TACN	1-dodecyl-1,4,7-triazacyclononane
C_{16}DPA	N,N-bis(pyridin-2-ylmethyl)hexadecan-1-amine
C_{12}DPA	N,N-bis(pyridin-2-ylmethyl)dodecan-1-amine
HEPES	(4-(2-hydroxyethyl)-1-piperazineethanesulphonic acid)

Contents

Abstract

Chemists and engineers have been attempting to miniaturise systems using microfluidics technologies for the past two decades. It has a number of advantages, including portability, high throughput due to parallelization, and a small amount of sample requirement. However, due to the high cost of fabricating a microfluidic chip and the complicated continuous flow control setup needed, this technology has yet to be adopted for large-scale societal applications. In this context, we attempted to develop a tool in which flow is produced within a closed microchamber as a result of specific interactions and catalysis, allowing disease-specific biomolecular recognition events to be detected in a much more straightforward and cost-effective manner. Herein we have made a micropump that can perform the catalysis of substrates like HPNPP and BPNPP .HPNPP is an RNA model substrate while BPNPP is DNA model substrate. Using these substrates, we have observed how there is change in flow of tracer particles when these substrates undergo hydrolysis. The substrates HPNPP and BPNPP contain phosphate group in them. Similar to phosphodiester bond cleavage in nucleic acid like DNA and RNA, in these substrates also the phosphodiester bond breaks. For the catalysis of these substrates, different kind of surfactants were synthesised.

The head group of the surfactants having metal ion shows better affinity towards phosphates. We have immobilised the surfactant having metal ion in its head group to a glass surface where the silver patch was already formed. The surfactant bonded to silver through metal-thiol bonding and the self–assembled monolayer thus formed was used for studying the flow of tracer particles. The flow was affected by the interactions between the self-assembled monolayer and the substrates. This self-assembled monolayer acted as a catalyst for hydrolysing HPNPP into PNP and cyclic phosphate and BPNPP into PNPP and PNP. We also used ATP for studying the multivalent interactions towards the self-assembled

monolayer. The catalysis of HPNPP and BPNPP was also monitored using the UV-vis. In future these kind of pumps can be used for DNA and RNA sensing and for diagnosing various diseases using real world samples which can be cost –effective and will require less time.

Chapter 1

Introduction

Fluids play a very vital role in nature. Flow of fluids is important for the sustenance of life on earth as life without fluidic motion would not have been possible. The motion of fluid has a very significant part in various aspects, be it motion of jellyfish in water, in running a vehicle ,in very large scales like in case of flow of water through dams or in small scale like the blood flow through arteries and veins ,flow of cytoplasm etc. [1] When considering the large scale flows and small scale flows (typically inside human cell),there are many factors that differ them like the Reynold's number which is typically low in small scale flows as compared to macroscale flows ,diffusion, surface tension and surface area to volume ratio which have a very important role in small scale flows.[2]

1.1 Microfluidics

Microfluidics is the field that deals with fluids that are typically constrained in a microscale typically in a microfluidic devices.[3] Microfluidics is used for the diagnosis of diseases like cancer, in DNA analysis [4] in drug delivery [5] and in cell manipulation [6], microfluidics has also been used for studying the flow inside human cells.[7] Microfluidics offer various advantages as it requires low sample/reagent volume which range from microliter to nanolitre ,low cost, high sensitivity to samples and less time requirement for performing the experiments.[3]

1.2 Micro pumps

Micro pumps are the devices in which small volume of fluid flow and the fluid flow can be controlled and monitored. Micropumps are categorized into two types –mechanical and non-mechanical pumps. [8] Mechanical pumps require an external energy source like electricity for pumping fluids and the non-mechanical micropumps do not require any external source for the pumping of fluid inside them and have simplistic design. One of the feature of non-mechanical micro pumps is that they respond to external stimuli whenever they are exposed, and this property is of great use as they can be used for making biosensors which are cost-effective.

Recently many self-powered chemical micropumps have been developed [9] which can respond to certain analytes .The idea of these micropumps was inspired from bimetallic nanomotors, which consisted of two metals, platinum and gold[10] and when the rods containing gold and platinum were dipped in solutions of H_2O_2 then the H_2O_2 was catalysed. The gold acted as cathode, whereas the platinum as anode. The catalysis of H_2O_2 led to generation of high proton concentration toward platinum side as compared to gold. This led to electric filed formation pointing from platinum to gold and these rods moved towards the platinum side. The H_2O_2 served as fuel for driving the motors.

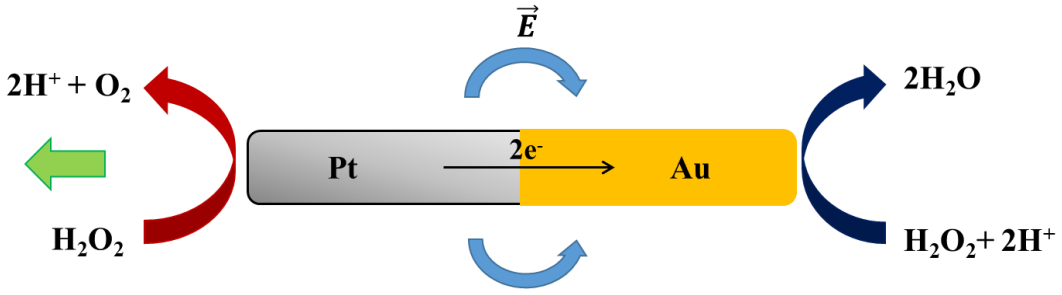

Figure 1: a bimetallic nanorod consisting of platinum and gold which move in H_2O_2 solution (*redrawn from 11*)

Owing to the above bimetallic nanorods Kline. *Et al.* made an Au-Ag catalytic pump where the Ag was deposited on the Au surface. The Ag acted as cathode and Au as anode .When H_2O_2 was added to this pump then decomposition of H_2O_2 [22] took place, the proton

moved from Au to Ag thus leading to flow generation. The major concern with catalytic micropumps were that they were not bio-compatible.

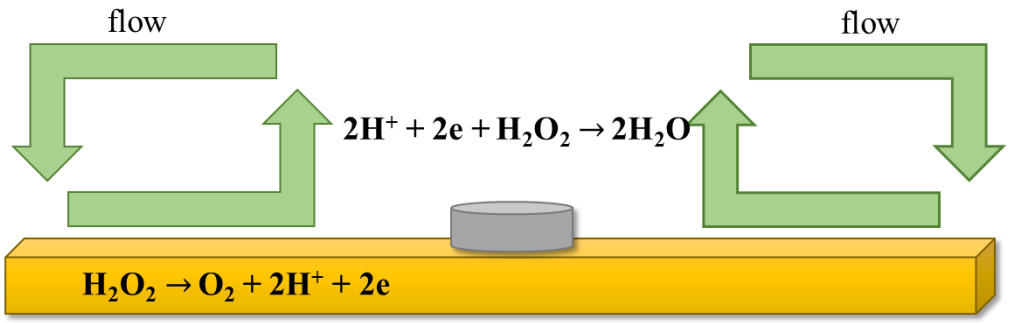

Figure 2: flow of tracer particles in Au-Ag micropump (*redrawn from 12*)

1.2.1 Self-powered-enzyme micropumps:

Recently many self-powered enzyme micropumps have been developed which were bio-compatible and they were based on the idea that, as the enzymes are substrate-specific and when these enzymes are immobilised on a surface, so they act as a catalyst for their particular substrate. The speed of these micropumps can be varied depending on the substrate concentration. Initially, the gold was immobilised on a Polyethylene glycol-glass surface. The gold surface was then coated with the quaternary ammonium thiol which formed a self-assembled monolayer on the gold surface.[13] The formation of the gold-sulphur bond acts as a driving force for the deposition of the thiolated compound on gold.[14] The negative charged enzymes were added which then were bonded to the self-assembled monolayer. The substrate and the tracer particles were added to the chamber and using the optical microscope the flow of tracer particles was observed.

A self–powered enzyme micropump was designed by Sengupta *et al.* [13] where on the gold-coated glass surface, the immobilisation of surfactant led to the formation of self-assembly monolayer and catalase enzyme was added to the top of this monolayer. After that the tracer particles along with glucose oxidase and glucose were added to the chamber. The production of H_2O_2 lead to the generation of flow such that the tracer particles moved inward. When the

slides were inverted, then the particles moved outward, demonstrating that it was a density-driven flow.

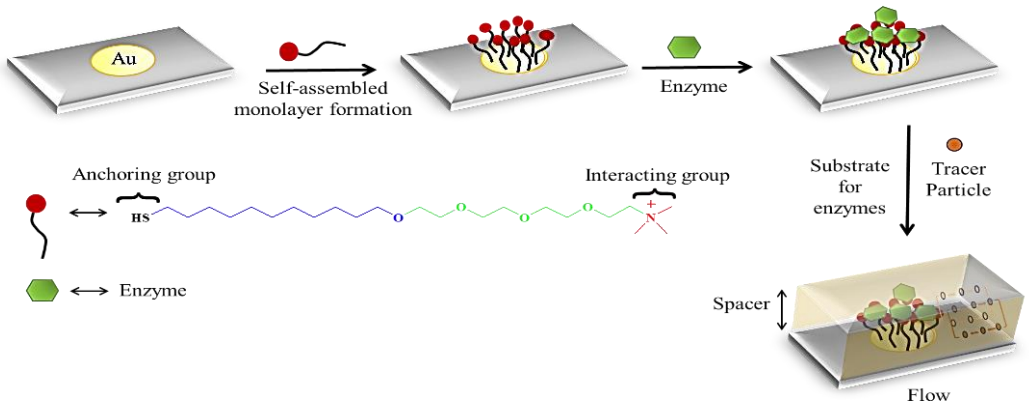

Figure 3: Schematic diagram of immobilisation of enzyme to the self-assembled monolayer and flow of tracer particles inside the micropump (*redrawn from 13*.)

A silver-based self-powered micropumps was made. One such pump was used as pH-sensitive pump[15] where in a glass slide having silver patch enzymes such as glucose oxidase was used to change the pH. This enzyme decomposes glucose to gluconic acid which is acidic and this change in pH led to fluid flow generation. This pump worked as a glucose sensor.[15] .Similar to the above mentioned self-powered enzyme micropump, here also when the slides were inverted then the direction of flow was inverted which showed that it was a density driven flow

Inspired from the above chemically powered enzyme micropumps we designed a micropump where we used synthetic catalyst for catalytically hydrolysing the DNA and RNA model substrates and flow generated due to the catalysis of these substrates was observed

Nucleic acids are important part of all organism that store the genetic information. In DNA and RNA .Phosphodiester bonds are formed between carbon atom at 3 position of 1 sugar and carbon atom at 5 position of other sugar. For studying the hydrolysis of nucleic acids like DNA and RNA there have been many phosphodiester compound synthesized that resemble to these nucleic acid. These compound are preferred over dinucleoside-3´, 5´-monophates as these dinucleoside-3´, 5´-monophosphates are very small, and the kinetic studies are a bit

difficult with them and so for studying the cleavage of Phosphodiester bond in RNA a similar type of compound (HPNPP) was used .[16]

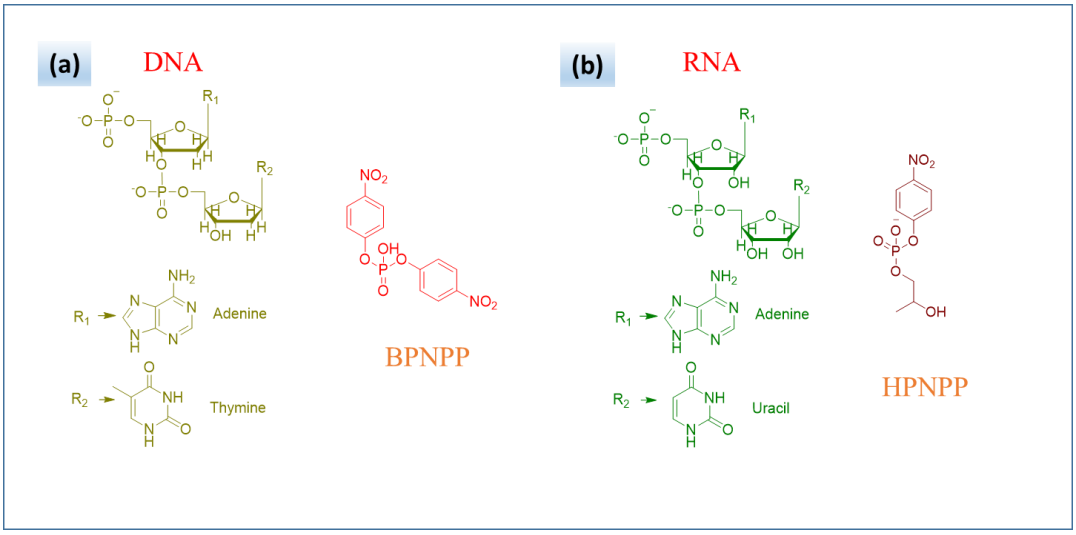

Figure 4: (a) chemical structure of DNA and its resembling model (BPNPP) ,(b) the chemical structure of RNA and its resembling model(HPNPP) (*redrawn from 17*)

At physiological pH the DNA phosphodiester linkages are very stable. Cleavage of Phosphodiester bonds can be carried out using complexes of metal ions .BPNPP is a compound that mimics DNA in having similar kind of phosphodiester linkage. Many metal chelating surfactants have been synthesized [18, 19, 20] which tend to form self-assembly on the surface of metal via metal-thiol bonding [18] or through a substrate like, in the catalysis of HPNPP the surfactant C_{16}TACN.Zn^{2+}act as a catalyst.[21] The TACN.Zn^{2+} moiety has better binding to HPNPP as it contains Phosphate group.[22] The critical assembly concentration of C_{16}TACN.Zn^{2+} is generally 50uM. When the concentration of substrate is increased then the critical assembly concentration deceases and thus the assemblies formed lead to catalysis of HPNPP thus forming cyclic phosphate and PNP .[21]

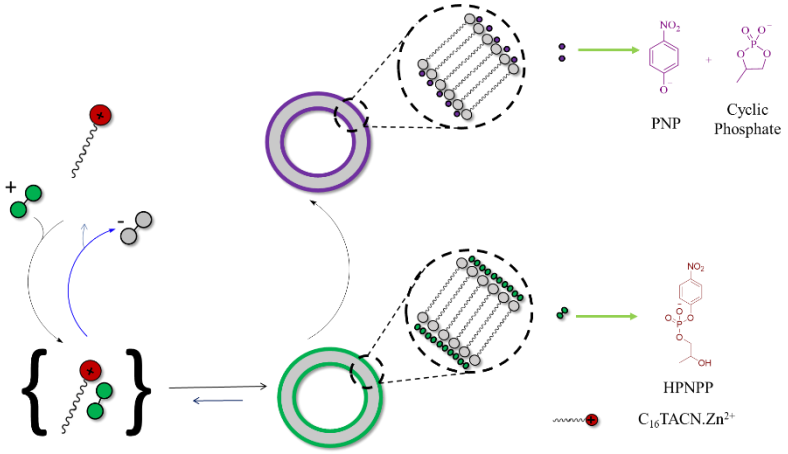

Figure 5: formation of self-assemblies of $C_{16}TACN.Zn^{2+}$ in presence of substrate HPNPP which leads to catalysis of HPNPP *(redrawn from 21).*

Mancin, Scrimin *et al*. have used metal-thiol bonding for catalysis of BPNPP wherein the catalyst thiolated ($BAPA.Zn^{2+}$) bind to solid surface(nanoparticle) in a solution and the self-assembly thus formed leads to catalysis of DNA model substrate –BPNPP. [23]

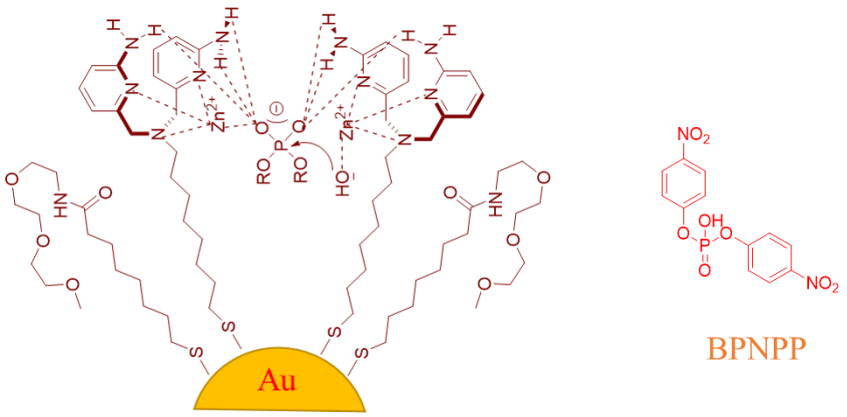

Figure 6: interaction of BPNPP with self-assembly of thiolated ($BAPA.Zn^{2+}$) surfactant with triethyleneglycol-terminated thiols (*redrawn from 23)*

For studying the catalysis in micropump, Initially, silver was deployed on a glass surface and then utilising the Metal-sulphur bonding specifically(Ag-S)bonding the thiolated compound having metal ion in its head group was added to the silver patch which formed a cationic self-assembled monolayer. The thiolated compound chosen was 9-(1, 4, 7-triazacyclononan-1-yl) nonane-1-thiol.[18] The metal ion chosen was such that it was non-toxic, redox-inactive and easily available.[23] We used zinc metal ion that bonded to the thiolated compound through non-covalent interactions. The main characteristics of this monolayer of alkyl thiol having head.

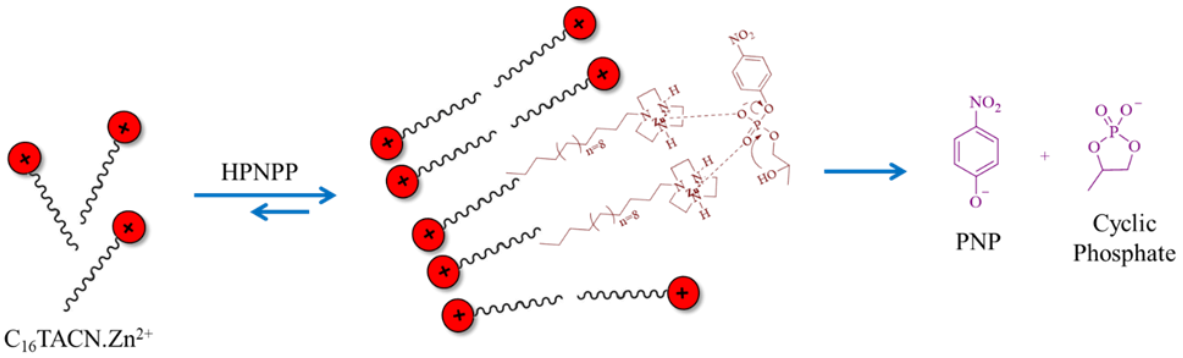

Figure 7: interaction of HPNPP to the self-assembly of surfactant which leads to product formation (*redrawn from 21)*

group as $TACN.Zn^{2+}$ is that the $TACN.Zn^{2+}$ has a higher binding affinity towards nucleotides and phosphates(binds the nucleotides and phosphates effectively).Thus the cationic monolayer of the thiolated compound acted as a catalyst for breaking of the phosphodiester bonds. Previous work has been reported which shows that when the compound $TACN.Zn^{2+}$ is in its isolated form then it cannot lead to transphosphorylation of HPNPP [18] as it requires two metal ions to do so. So, the formation of catalytic self-assembled monolayer lead to the generation of multivalent system [27] which could effectively lead to transphosphorylation of HPNPP. The catalysis of HPNPP leads to the generation of cyclic phosphate and PNP, whereas catalysis of BPNPP gives PNPP and PNP in a similar fashion to HPNPP. So, the flow generated due to catalysis can be helpful for understanding the

directional motion of genetic material, organelles and nutrients in the cell which is influenced by the flow of cytoplasm.[24]

Chapter 2

Experimental Setup and Methods

This chapter describes experimental techniques and procedures involved to study the catalysis of substrates (HPNPP and BPNPP)

2.1 Experimental Methods:

2.1.1 UV-Vis Spectroscopy: Using Varian Cary 60 (Agilent technologies) spectrophotometer, UV-Vis studies were carried out. The catalysis of substrates was carried out by following the product formation at 400 nm. Total reaction volume in the cuvette was fixed at 1 ml and for kinetic study a cuvette of 1 cm path length was used. All measurements have been performed at 25 ^{o}C.

2.1.3 Nuclear magnetic resonance spectroscopy: For recording the NMR spectra Bruker Avance-III 400 MHz spectrometer was used. ^{1}H and ^{13}C NMR were recorded at operation frequencies 400 MHz and 100 MHz, respectively. $CDCl_3$ and DMSO-d6 were used as the solvents and tetramethylsilane (TMS) as the internal standard for recording the samples. The chemical shift values are reported as delta (δ) units in parts per million (ppm).

2.1.4 Optical and Fluorescent microscopy: The flow of tracer particles was observed using Zeiss Axis Observer 7 microscope having Axio Cam 503 Mono 3 Megapixel with ZEN 2 software. For monitoring the flow of tracer particles, the movies were recorded in the microscope, keeping the lens at 20x and frame rate at nearly 5fps. Movies of 30 seconds were recorded for 2, 5 and 10 minutes and then using tracker software the velocity of particles was calculated.

2.2 EXPERIMENTAL PROCEDURES:

2.2.1 Synthesis of C_{16}TACN:

2.2.1.1 Synthesis of TACN-DiBoc:

Synthesis of compound was carried out as per literature.[18] Compound **1A** [TACN] (0.2g, 0.8382mmol) was mixed with DBU (0.612g, 4.024mmol) in Chloroform (25ml). Boc_2O(0.4g,1.844mmol) was solubilised in anhydrous Chloroform(5ml).[12] At room temperature, the solution of Boc_2O was added to the solution of compound **1A** using a syringe pump(0.5ml/hr) under an inert(nitrogen) atmosphere and the resulting solution was then stirred for 36hrs. Then the organic layer was washed using chloroform (100ml) and a saturated solution of $NaHCO_3$. Using rota evaporator, solvent evaporation was done, and later column chromatography (2%Methanol in DCM) was performed and compound 1**B** [TACN-Diboc] (0.09g) was obtained as a viscous yellow oil.

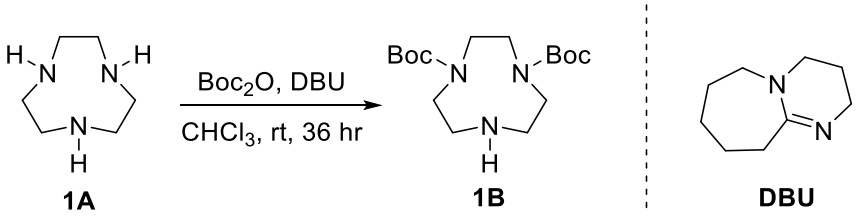

Scheme 1.1

2.2.1.2 Synthesis of C_{16}TACN-DiBoc:

The Compound was synthesised as per literature.[19] The suspension of K_2CO_3 (0.112g, 0.81138mmol) and $NaHCO_3$ (0.068g, 0.81138mmol) was prepared in MeCN (20ml). Compound **1B[**TACN-Diboc] (0.09g, 0.27319mmol) and **1C** [$C_{16}H_{33}Br$] (0.1g, 0.32783mmol) were added to the above suspension and the resulting solution was stirred at 60° C for 3 hrs .Then the filtration was carried out and the solvent was evaporated to obtain a crude product and column chromatography (silica gel: 1%Methanol/DCM) was used to purify the product. Compound 1**D [**C_{16}TACN-Diboc**]** (0.080g) was obtained as a pure product.

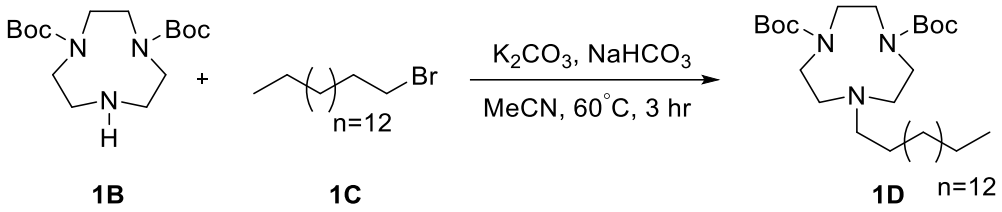

Scheme 1.2

2.2.1.3 Deprotection of C_{16}TACN-DiBoc:

The Compound was synthesised as per literature.[19] MeOH (4ml) and HCl (6M, 4ml) were added to Compound **1D** (0.08 g, 0.144 mmol). The resulting solution was continuously stirred for 5 hrs at 60 °C. The solvent was evaporated using a rotatory evaporator and then the compound **1E** [C_{16}TACN] was completely dried using high vacuum. Pure **1E** (0.034g, 51% yield) was obtained as a white powder. ^{1}H NMR (400 MHz, D_2O); 3.46 (s_{br}, 4H), 3.20 (s_{br}, 4H), 2.89 (s_{br}, 4H), 2.64 (s_{br}, 2H), 1.40 (s_{br}, 2H), 1.10 (s_{br}, 26H), 0.69 (s_{br}, 3H). ^{13}C NMR; 47.40, 43.10, 41.75, 31.98, 30.08, 29.55, 22.62, 13.86

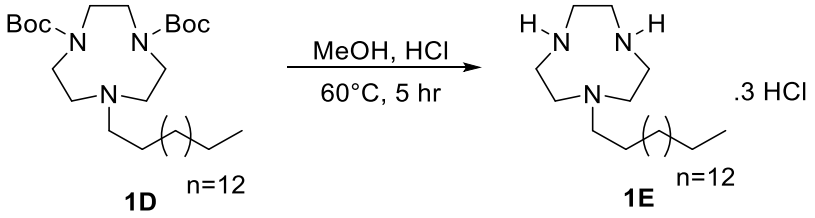

Scheme 1.3

2.2.2 Synthesis of TACN-SH

2.2.2.1 Synthesis of S-9-Br:

The Compound was synthesised as per literature.[18] Compound **2A** [1, 8-Dibromononane] (1.25 g, 4.378 mmol) was dissolved in 30 ml of acetone. To the above solution, Potassium thioacetate (0.5 g, 4.378 mmol) was added. For 12 hrs, the resulting solution was stirred under an inert atmosphere (nitrogen). Then filtration was done of the resultant suspension

and using rota evaporator solvent evaporation was carried out. The Compound was dried using high vacuum. Column chromatography (2% ethyl acetate/hexane) was performed. Pure compound **2B**[S-9-Br] (0.8g) was obtained as a colourless oil which was used for further reactions.

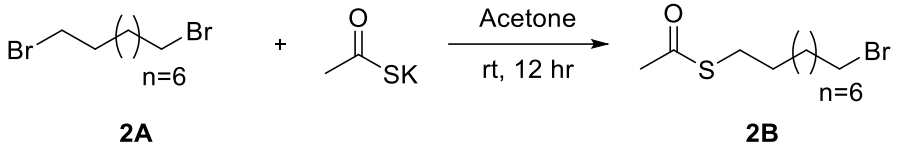

Scheme 1.4

2.2.2.2 Synthesis of TACN-DiBoc:

Synthesis of the compound was carried out as per literature.[18] Compound **1A** (0.2g, 0.8382mmol) was mixed with DBU (0.612g, 4.024mmol) in Chloroform (25ml).Boc_2O (0.4g, 1.844mmol) was solubilised in anhydrous Chloroform (5ml). At room temperature, the solution of Boc_2O was added to the solution of compound **1A** using a syringe pump (0.5ml/hr) under an inert (nitrogen) atmosphere and The resulting solution was then stirred for 36hrs and then the organic layer was washed using chloroform (100ml) and saturated solution of $NaHCO_3$.Using rota evaporator, solvent evaporation was done and later column chromatography (2% methanol/DCM) was performed and compound **1B** (0.17 g) was obtained as a viscous yellow oil.

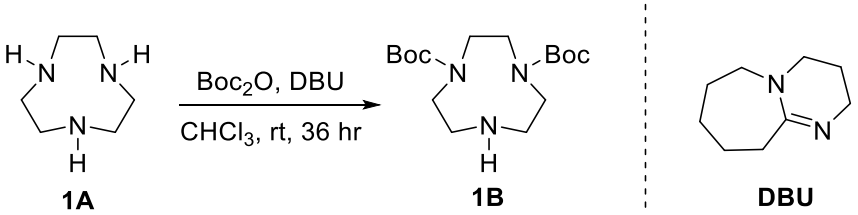

Scheme 1.1

2.2.2.3 Synthesis of S-9 TACN-DiBoc:

Synthesis of the compound was done as per literature.[18] the suspension of K_2CO_3 (0.211g, 1.532mmol) and $NaHCO_3$ (0.128g, 1.532mmol) was prepared in MECN (20ml). Compound **1 B** (0.17g, 0.5160mmol) and (**2B**) (0.174g, .6194mmol) were added to the above suspension and at 60° C the resulting solution was stirred for 3 hrs. Then the filtration was carried out and the solvent was evaporated to obtain a crude product and using column chromatography (silica gel: 1%Methanol/DCM), the compound was purified.NMR analysis was done. Compound **2C**[S-9-TACN-Diboc] (0.16g) was obtained as a pure product.

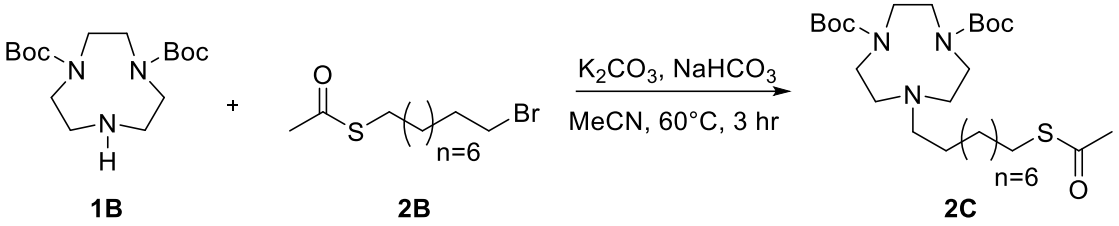

Scheme 1.5

2.2.2.4 Deprotection of TACN S-9 DiBoc:

The Compound was synthesized as per literature.[18] MeOH (4ml) and HCl (6M, 4ml) were added to Compound **2C** (0.16g, 0.3022mmol) .The resulting solution was continuously stirred for 5 hrs at 60° C using reflux .The solvent was evaporated using rotatory evaporator and then the compound **2D** was completely dried using high vacuum .Pure compound **2D** [TACN-SH] (0.095g, 79% yield) was obtained as white powder. ^{1}H NMR (400 MHz, D_2O); 3.29 (s_{br}, 4H), 3.21 (s_{br}, 4H), 3.14-3.12 (s_{br}, 4H), 2.86-2.82 (m, 2H), 2.37 (t, 2H), 1.48-1.41 (m, 4H), 1.15 (sbr,12H).^{13}C NMR ; 56.08,48.31,42.09,41.92,41.78,32.98,28.39,28.26,28.00,27.39,26.07,23.71

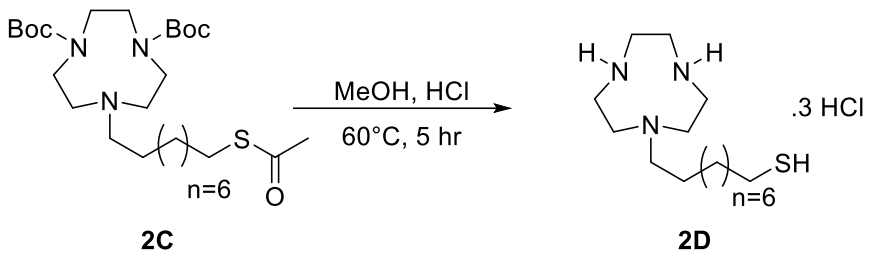

2C **2D**

Scheme 1.6

2.2.3 Synthesis of DPA-SH

2.2.3.1 Synthesis S-9-DPASOCH$_3$:

As per literature[25] K_2CO_3 (0.083g, 0.6mmol) was mixed with KI (0.02g, 0.12mmol) in acetone (20ml) and **2B** (0.084g, 0.3mmol) was added to the above solution. **3A** [DPA] (0.1g, 5mmol) was solubilized in acetone (5ml). The solution of **3A** was added to the solution of (**2B**) (using a syringe pump). The stirring of the resulting solution was carried out for 20 hrs at 45°. Filtration was done and the solvent was evaporated using rota evaporator. The compound was dried using high vacuum. Column chromatography (90% ethyl acetate/hexane) was done for purifying the compound. Compound **3B**[S-9-DPASOCH$_3$] (0.07g, 0.175mmol) was obtained as a dark brown oil.

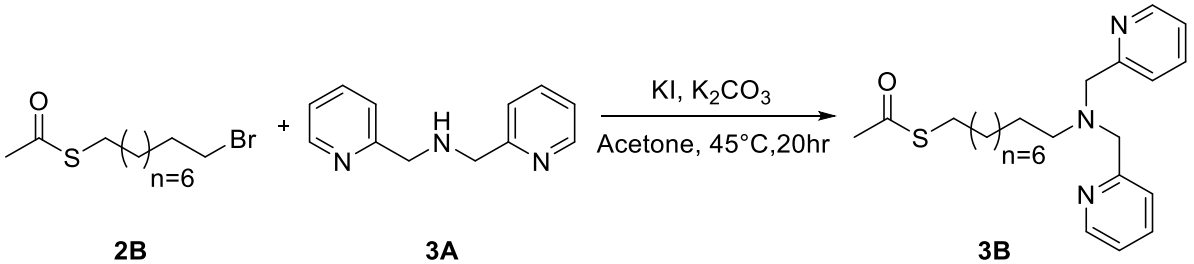

2B **3A** **3B**

Scheme 1.7

2.2.3.2 Synthesis of DPA-SH:

Synthesis of the compound was done as per literature. [26] Compound **3B** (0.07g, .175mmol) was added to ethanol (10ml) in inert atmosphere. Then NaOH (0.01438g, 0.3595mmol) solution was prepared in H_2O (2ml). The solution of NaOH was added dropwise to the solution containing Compound **3B**. The resulting solution was stirred and for 2hrs at 78°C using reflux and then it was allowed to cool. The solution was then neutralised using 2M HCl (6ml) and in separation funnel the solution was then transferred under an inert atmosphere. In the separation funnel 10 ml of nanopure water and 20 ml of diethyl ether were added. Using Na_2SO_4 the organic layer was dried and then was collected in a round bottom flask. The solvent was evaporated using a rota evaporator and the compound was dried using high vacuum. Pure compound **3C** [DPA-SH] (0.05g, 80% yield) was obtained as a dark brown oil. ^{1}HNMR (400 MHz, CDCl3); 8.54 (d, 2H), 7.71-7.67 (m, 2H), 7.58(d, 2H), 7.18(t, 3H), 3.92(s, 4H), 2.69-2.62(m, 4H), 1.69-1.62(m, 2H), 1.58(m, 2H), 1.35-1.23(s_{br}, 10H) **.** ^{13}C NMR; 148.73, 136.68, 123.59, 122.00, 60.27, 54.15, 39.23, 29.71, 29.39, 29.18, 28.48, 27.12

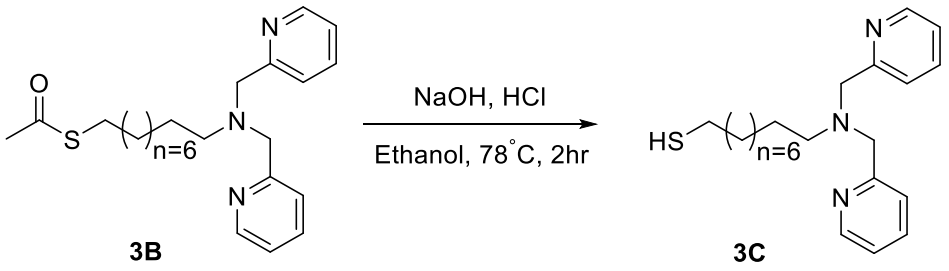

Scheme 1.8

2.2.4 Synthesis of C_{12}TACN

2.2.4.1 Synthesis of TACN-DiBoc:

The synthesis of the compound was carried out as per literature. [18] Compound **1A** (0.2g, 0.8382mmol) was mixed with DBU (0.612g, 4.024mmol) in Chloroform (25ml).Boc_2O (.4g, 1.844mmol) was solubilised in anhydrous Chloroform (5ml). At room temperature, the solution of Boc_2O was added to the solution of compound **1A** using a syringe pump

(0.5ml/hr) under an inert (nitrogen) atmosphere and The resulting solution was then stirred for 36hrs and then the organic layer was washed using chloroform (100ml) and saturated solution of $NaHCO_3$.Using rota evaporator, solvent evaporation was done and later column chromatography (2%methanol/DCM) was performed and compound **1B** (0.11g) was obtained as a viscous yellow oil.

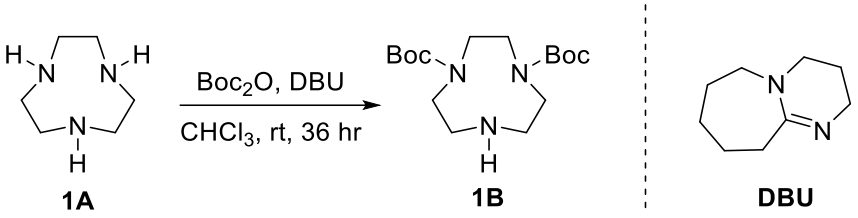

Scheme 1.1

2.2.4.2 Synthesis of C_{12}TACN-DiBoc:

The Compound was synthesised as per literature.[21] the suspension of K_2CO_3 (0.137g, 0.99168mmol) and $NaHCO_3$ (0.083g, 0.99168mmol) was prepared in MeCN (20ml). Compound **1B** (0.11g, 0.27319mmol) and **4A** [$C_{12}H_{25}Br$] (0.122g, .0.400mmol) were added to the above suspension and the resulting solution was stirred at 60° C for 3 hrs .Then the filtration was carried out and the solvent was evaporated to obtain a crude product and using column chromatography (silica gel: 1%Methanol/DCM), the compound was purified.NMR analysis was done. Compound **4B** [C_{12}TACN-Diboc] (0.080g) was obtained as a pure product.

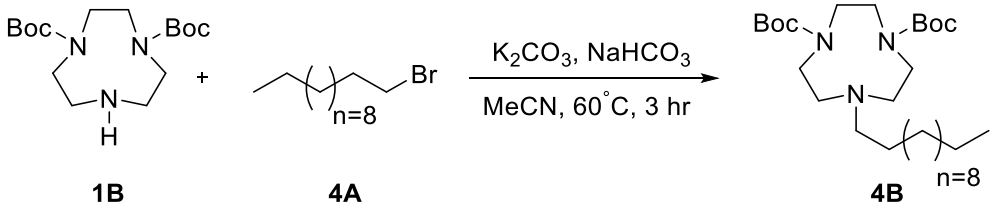

Scheme 1.9

2.2.4.3 Deprotection of C_{12}TACN-DiBoc:

The Compound was synthesised as per literature.[21] MeOH (4ml) and HCl (6M, 4ml) were added to Compound **4B** (0.08g, 0.160mmol) .The resulting solution was continuously stirred for 5 hrs at 60° C. The solvent was evaporated using a rotatory evaporator and then the compound **4C** was completely dried using high vacuum. Pure **4C** [C_{12}TACN] (0.032g, 49% yield) was obtained as white powder. . ^{1}H NMR (400 MHz, D_2O); 3.45(s, 4H), 3.23(s, 4H), 2.95(s_{br}, 4H), 2.69(s_{br}, 2H), 1.44(s, 2H), 1.13(s, 18H), 0.72(t, 3H).

^{13}C NMR; 47.51, 42.93, 41.75, 31.87, 29.79, 29.38, 27.26, 24.02, 22.56, 13.85

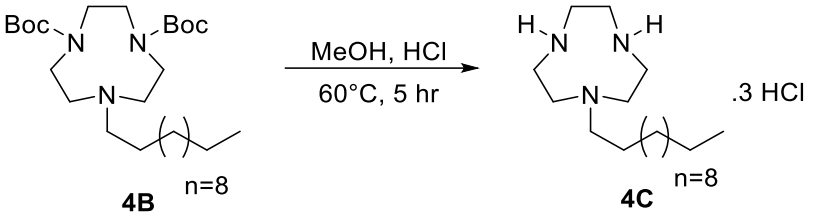

Scheme 1.10

2.2.5 Synthesis of C_{16}DPA

As per literature[20] **3A** (0.1 g, 0.502 mmol), **1C** (0.153g, 0.502mmol) and K_2CO_3 (0.207g, 1.5mmol) were added to acetonitrile. The resulting mixture was continuously stirred for 26hrs using reflux .Then the solution was allowed to cool and using rota evaporator solvent was evaporated .Then Column chromatography (90% ethyl acetate /hexane) was performed. Compound **5A** [C_{16}DPA] was obtained as pure product (0.08g, 38% yield) ^{1}H NMR; 8.54(d, 2H), 7.70-7.61(mbr, 4H), 7.18(d, 2H), 3.92(s, 4H), 2.62(s, 2H), 1.60(sbr, 2H), 1.30-1.22(s, 26H), 0.89(t, 3H)

^{13}C NMR; 160.19, 148.91, 136.36, 122.81, 121.84, 60.49, 54.52, 31.94, 29.71, 29.68, 29.63, 29.50, 29.38, 27.33, 27.09, 22.71, 14.15.

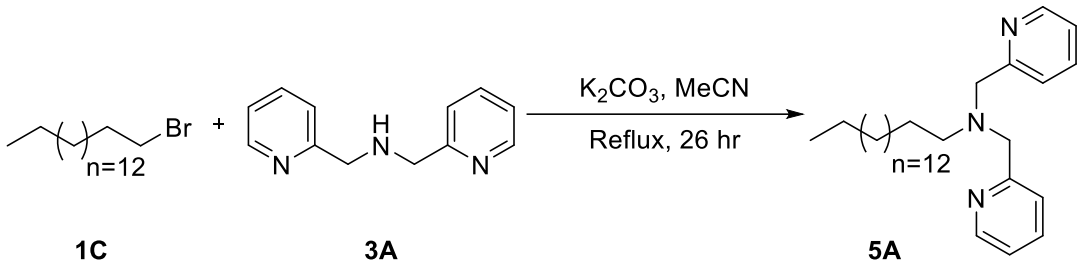

Scheme 1.11

2.2.6 Synthesis of C_{12}DPA

Synthesis of compound was done as per literature.[20] **4A** (0.062 g, 0.251 mmol), **3A** (0.05g, 0.2521mmol) and K_2CO_3 (0.104g, 0.753mmol) were added to acetonitrile. Continuous stirring of resulting mixture was done for 26hrs using reflux The resulting mixture was continuously stirred for 26hrs using reflux .Then the solution was allowed to cool and solvent was evaporated using rotatory evaporator .Then Column chromatography (90% ethyl acetate /hexane) was performed. Compound **6A** [C_{12}DPA] (0.04g, 43.1% yield) was obtained as pure product. ^{1}H NMR; 8.55(d, 2H), 7.72-7.68(mbr, 4H), 7.21(t, 2H), 4.00(s, 4H), 2.69(s, 2H), 1.64(sbr, 2H), 1.27-1.23(s, 18H), 0.89(t, 3H) , ^{13}C NMR; 160.20, 148.91, 136.37, 122.81, 121.84, 77.35, 76.72, 60.50, 54.53,31.93,29.64, 29.50, 29.37, 27.33, 27.09, 22.71, 14.15.

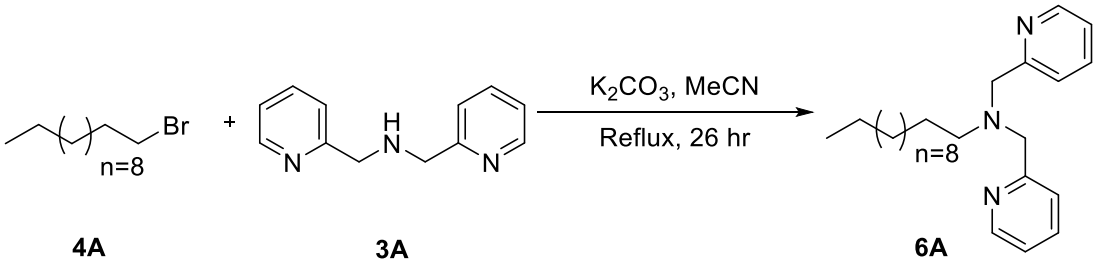

Scheme 1.12

2.3 Designing of Micropump-

2.3.1 Fabrication of glass slide:

The deposition of silver on a glass slide was done using the previous literature procedure.[25] Initially 100mM $AgNO_3$ solution, 3mM NaOH solution and 0.5 mM glucose solution were prepared in nanopure water. All the solutions were taken in different vials. Then 500µL of $AgNO_3$ solution was taken in a separate vial and to the vial containing $AgNO_3$ solution, 30-35µL ammonia solution was added in increments till the solution was clear and to this solution, 1µL of 3mM NaOH solution was added. The resulting solution was tollens [Ag $(NH_3)_2$] reagent. Then 2µL of Tollen's reagent was added to glass slides, and 6µL of 0.5mM glucose solution was added to the slide containing Tollen's reagent. After 15-20 minutes, the colour of the solution changed to silver. Then the slides were dried for a day and then were washed with water.

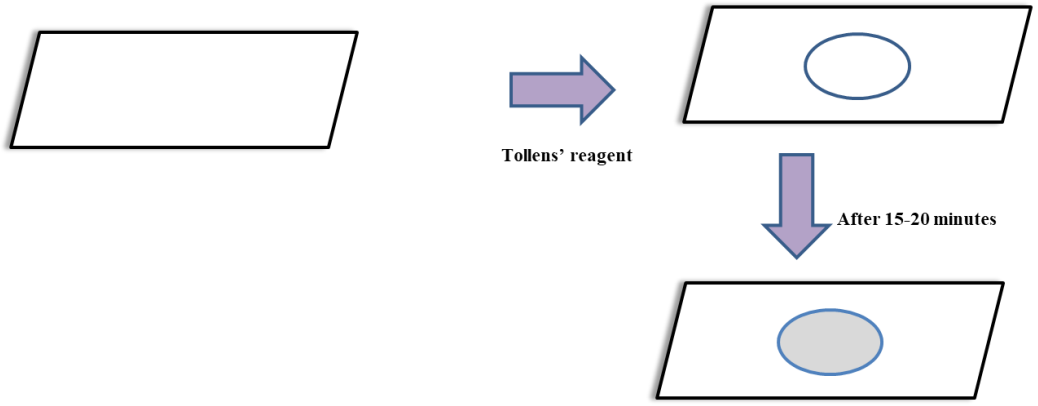

Figure 8: Schematic diagram of deposition of silver on the glass slide

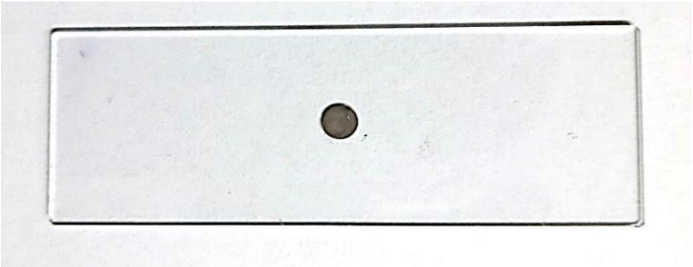

Figure 9: the image of a glass slide having a silver patch

2.3.2 Deposition of organic interface:

Thiolated surfactant 2D (9-(1, 4, 7-triazacyclnonan-1-yl) nonane-1-thiol) was used here for the formation of a self-assembled monolayer. Solutions of thiolated surfactant(5mM) and zinc nitrate (5mM) was prepared in 5mM HEPES buffer (pH=7) separately. After that, the solution of thiolated compound and zinc nitrate were mixed in equal proportion in a vial. The resulting solution was kept for some time so that the zinc gets encapsulated inside the moiety of TACN through non-covalent interactions. Then 15µL of the resulting solution was taken and added to the glass slide containing the silver patch. The slide was then washed with nanopure water and then it was covered with a closed hybridisation chamber of 20mm diameter and having 0.8mm height. The solutions to be analysed were added to the microchamber.

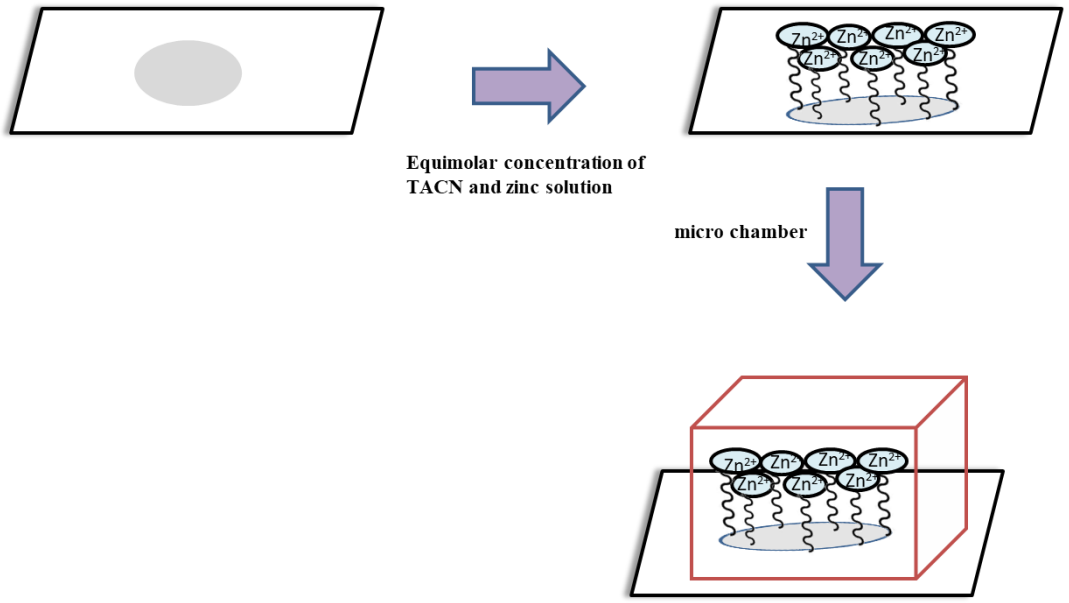

Figure 10: Schematic diagram of deposition of surfactant on the glass slide having a silver patch covered with microchamber

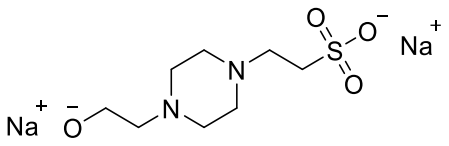

Figure 11: represents the structure of the HEPES Buffer

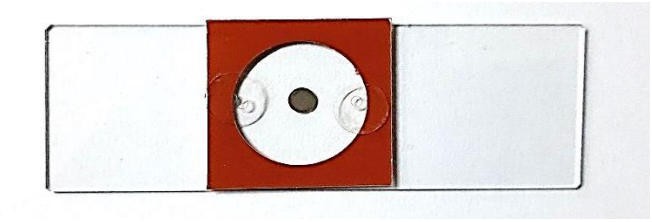

Figure 12: the image of the microchamber on the glass slide having silver patch.

Chapter 3

Results and Discussions

3.1 Catalysis of HPNPP (RNA model substrate) and BPNPP (DNA model substrate) by using UV-kinetics

A stuy by Leonard J.prins *et al.* [9] showed that substrates like HPNPP can lead to the formation of non-covalent self-assembly of various surfactants that can bind zinc metal ion. These self –assemblies act as a catalyst for substrate cleavage.

Here we have observed the rate of catalysis of HPNPP and BPNPP using surfactants with metal ion preferably zinc. HPNPP cleaves to yellow coloured PNP and Cyclic phosphate and BPNPP cleaves to form PNP and PNPP. Stock solutions of HPNPP (50mM) and BPNPP (50mM) were prepared in nanopure water. The catalysis was done using a UV-Vis spectrophotometer.

3.1.1 Catalysis of substrates using surfactant (C_{16}TACN.Zn^{2+}):-

We used the surfactant (C_{16}TACN) along with metal ion to observe the catalysis of HPNPP, BPNPP. A stock solution of C_{16}TACN (5mM) and zinc nitrate (5mM) was prepared in HEPES buffer (5mM, pH=7). The concentration of C_{16}TACN and zinc nitrate were in an equimolar ratio for the catalysis of HPNPP (500µM). Firstly the baseline was done using 100µM C_{16}TACN and 100µM zinc along with 5mM HEPES buffer. Then 500µM HPNPP was added to the cuvette and then catalysis of HPNPP was monitored at 400 nm and the concentration of Product PNP obtained was calculated. Similarly for BPNPP the same

procedure was followed and there was no significant catalysis of BPNPP even after 12 hours' time period.

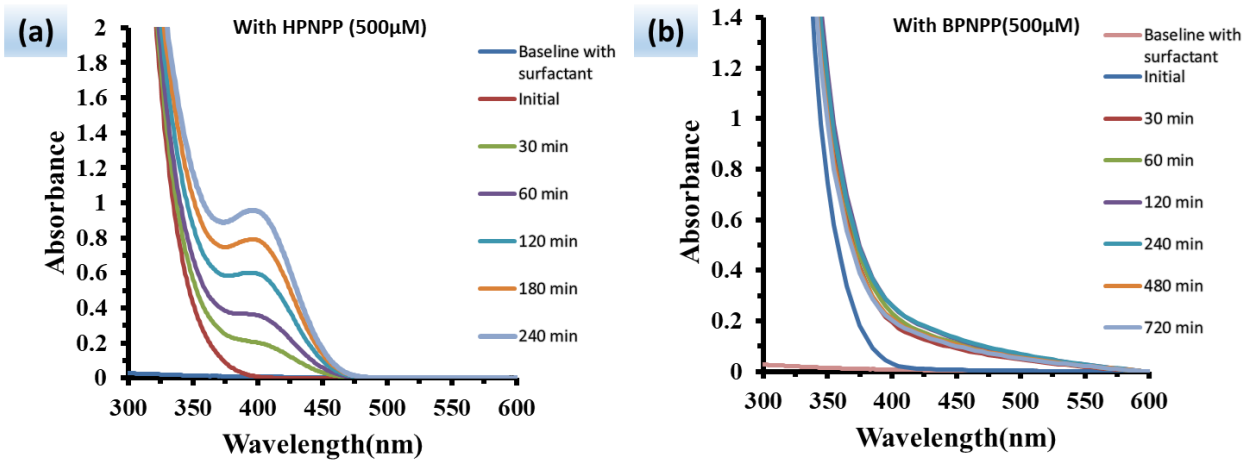

Figure 13: catalysis **(a)** of HPNPP (500µM) and **(b)** BPNPP (500µM) when the surfactant (C_{16}TACN.Zn^{2+}) was used . Experimental conditions: HEPES buffer (pH=7, 5mM), 25°C.

3.1.2 Effect of ATP on catalysis of substrates using surfactant (C_{16}TACN.Zn^{2+}):-

A stock solution of ATP (10mM) was prepared in nanopure water. 100µM of solution of (C16TACN) and zinc nitrate was added to the vial and to the same vial 100µM of ATP was added. The incubation of the resulting solution was done for 15 min .Then the baseline was done using 100µM surfactant (C_{16}TACN) and 100µM zinc along with 5mM HEPES buffer and then UV-data was recorded after adding HPNPP (500µM) solution. The UV scan were taken for different time periods. There was decay in the rate of catalysis of HPNPP. When the same procedure was carried out with BPNPP then very small changes in concentration were there in presence of ATP. The decay in the catalysis rate of HPNPP in the presence of ATP confirms that there is an interaction between surfactant and ATP, i.e. ATP gets assembled on the surface of surfactant, so the head group of surfactant is no more available to catalyse the substrates

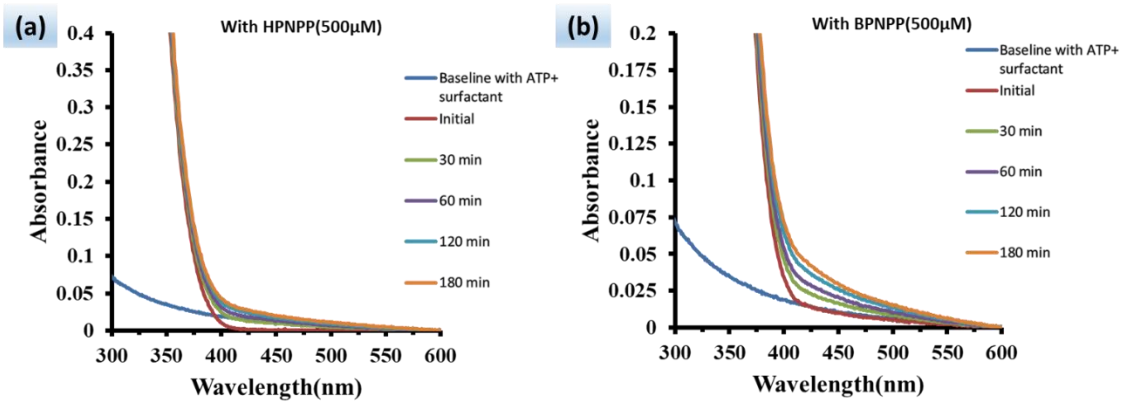

Figure 14: effect of ATP on the rate of catalysis of **(a)** HPNPP (500µM) and **(b)** BPNPP (500µM) in the presence of surfactant (C_{16}TACN.Zn^{2+}). Experimental conditions: HEPES buffer (pH=7, 5mM), 25°C.

3.2 Micropump flow Analysis:

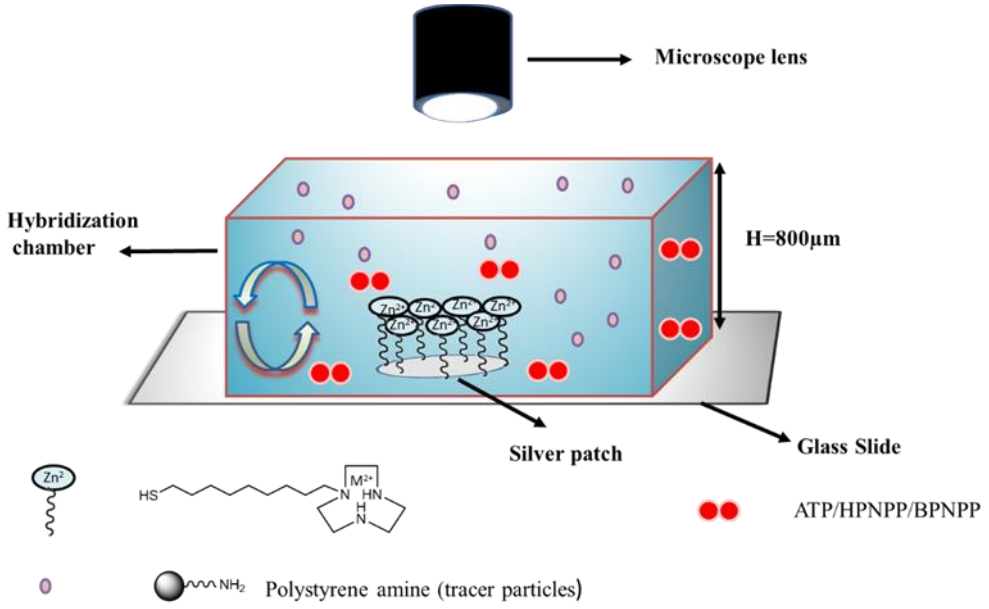

Figure 15: Schematic diagram of the flow of tracer particles observed through a microscope

Initially, on the glass slide having silver patch 5mM HEPES buffer solution with tracer particles (polystyrene amine beads having 2µm size) was added to the microchamber, and the flow of tracer particles was observed in the microscope. The velocity of tracer particles was calculated and it was found that velocity was (0.09 ± 0.04) µm/sec.Then another solution of nanopure water with tracer particles was prepared. In this case, tracer particles were prepared in nanopure water. This solution was added to the glass slide having surfactant immobilised on a silver patch. There was nearly no flow of tracer particles, and the velocity was found to be (0.28 ± 0.20)µm/sec.Then buffer solution along with tracer particles was added to the slide, having immobilised surfactant on the silver patch. The flow of tracer particles as observed in the microscope was outwards. The velocity found was (2.97 ± 0.83) µm/sec. This flow of tracer particles is due to the interaction of HEPES buffer with a surfactant which leads to the removal of sodium nitrate. Since the density of sodium nitrate is higher than HEPES buffer, so the flow is density-driven flow. The density of sodium nitrate= 2.26g/cm^3, Density of HEPES buffer=1.07g/cm^3, the difference in density of both these leads to the formation of flow.

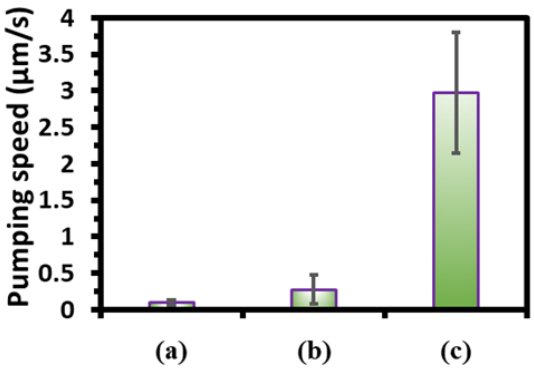

Figure 16: the velocity of tracer particles(average of 10 particles) on **(a)**glass slide having only silver patch Experimental Condition: HEPES buffer(pH7, 5mM), 25ºC.**(b)** glass slide having immobilised surfactant (TACN-SH.Zn^{2+}) Experimental Condition: nanopure water, 25ºC.**(c)** glass slide having surfactant (TACN-SH.Zn^{2+}) immobilised on the silver patch. Experimental Condition: HEPES buffer (pH7, 5mM), 25ºC.

3.2.1 Interaction of Phosphates with Surfactant:

Next, we tried to observe the supramolecular interaction between the nucleotides and surfactant (immobilised on Ag patch), but the flow obtained was similar to flow in the only buffer, so then we analysed the catalysis of bio mimicking substrates such as HPNPP, BPNPP. The flow of tracer particles was recorded in the presence of BPNPP only, HPNPP only, ATP only, HPNPP+ATP. The stock solutions of BPNPP, HPNPP, and ATP were in nanopure water and amine-modified tracer particles (2µm) were in HEPES buffer (5mM, pH7). For the flow, the concentration of substrate and nucleotide used was 500µM. It was observed that in the case of BPNPP, ATP, HPNPP+ATP, the flow of tracer particles was outward. However, in the case of HPNPP, the flow velocity of particles was inward. Velocity of Tracer particles in solution having-BPNPP: (0.97±0.40) µm/sec, HPNPP: (-0.80±0.52) µm/sec, ATP: (0.40±0.27) µm/sec, HPNPP+ ATP: (1.07±0.27) µm/sec (-ve sign implies inward flow + sign implies outward flow).

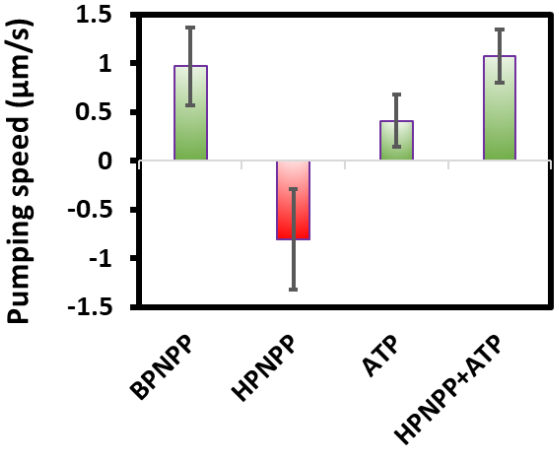

Figure 17: shows the velocity of tracer particles after 5 minutes when solutions of BPNPP (500µM), HPNPP (500µM), ATP (500µM), HPNPP (500µM) +ATP (500µM) were added to the glass slide having surfactant immobilised on silver patch. Experimental Condition: HEPES buffer (pH7, 5mM), 25ºC

.

3.2.2 Inward flow of HPNPP:-

Then the Stock solution of HPNPP (50mM) was prepared in nanopure water and the solution, along with tracer particles, was transferred to the glass slide having surfactant on the silver patch. The flow of tracer particles was recorded for 2,5 and 10 minutes and the flow velocity was found to be (-1.38±0.88)µm/sec(inward) for 2 minutes, (-0.80±0.52)µm/sec(inward) for 5 min (-0.31±0.37)µm/sec(inward) for 10 minutes and it was observed that with time the flow velocity decreases.

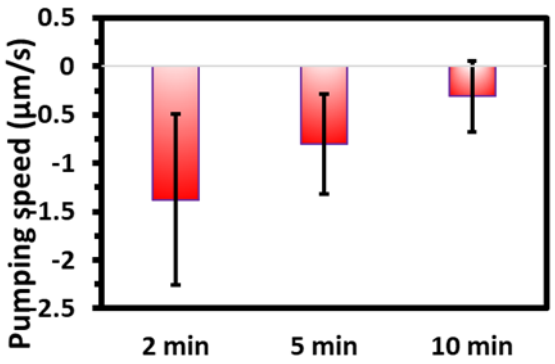

Figure 18: the inward flow velocity of tracer particles (average of 10 particles) after 2, 5 and 10 minutes when the solution of HPNPP (500µM) is added to the glass slide having surfactant immobilised on silver patch. Experimental Condition: HEPES buffer (pH7, 5mM), 25ºC.

3.2.3 Scanning spectra of solutions taken from microchamber:

The solution of HPNPP (500µM) along with tracer particles was added to the glass slide having immobilized surfactant and another solution of HPNPP (500µM) and ATP (500µM) along with tracer particles was added to other glass slide with immobilized surfactant. After 1 hour the solution were taken out and using UV-spectroscopy it was found that in case of solution having only HPNPP there was a peak at 400nm confirming that PNP was being

formed while in case of solution of ATP + HPNPP it was found that there was no peak at 400nm.

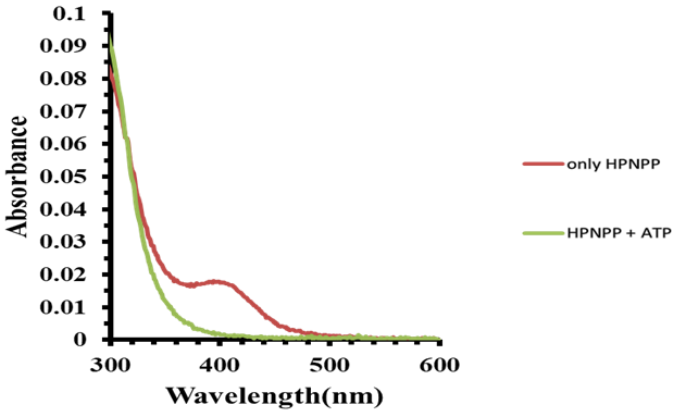

Fig 19: the catalysis of HPNPP (500uM) and effect of ATP on HPNPP catalysis when the solution from micro chamber were pipetted out

3.2.4 Outward flow of BPNPP:-

Similarly, the stock solution of BPNPP(50mM) was prepared and this solution, along with tracer particles, was added to the slide of the silver patch having immobilised surfactant, and the flow of tracer particles was recorded after 2,5 and 10 minutes. The flow of tracer particles was outward. The flow velocity calculated was (2.00±0.12) µm/sec (outward) for initial 2 minutes, (1.00±0.40) µm/sec (outward) for 5 minutes and (0.71±0.39) µm/sec (outward) for 10 minutes.

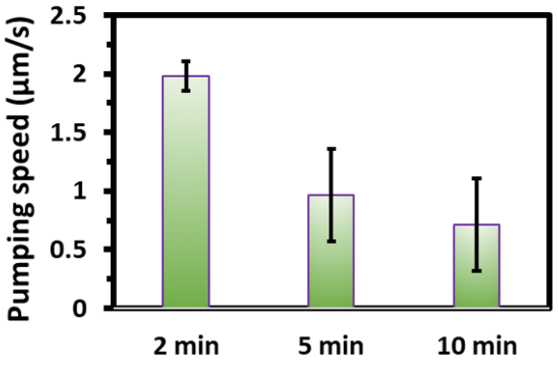

Figure 20: the outward flow velocity of tracer particles (average of 10 particles) after 2, 5 and 10 minutes when the solution of BPNPP (500µM) along with tracer particles is added to the glass slide having surfactant immobilised on silver patch. Experimental Condition: HEPES buffer (pH7, 5mM), 25ºC.

CONCLUSION

We have investigated the catalysis of HPNPP and BPNPP with the surfactants having a head group of TACN .Upon analysing the UV –kinetics data it was found that after 3 hours the catalysis of HPNPP was 3 folds greater than the BPNPP in the solution of C_{16}TACN.Zn^{2+}.Due to binding of ATP to the Surfactant C_{16}TACN.Zn^{2+} the catalysis of HPNPP was inhibited while there were very less changes in the catalysis of BPNPP

Here we showed a catalytically driven microscale fluid pump and showed that fluid flow direction could be controlled using different substrates. For studying catalysis in a microchamber, we used the thiolated surfactant having TACN head group was used. We used ATP for observing the multivalent interaction and it was found that the speed of tracer particles in the presence of ATP was less (similar to buffer) and outward. So next, we analysed the catalysis of HPNPP and BPNPP and it was found that the velocity of tracer particles in the presence of HPNPP was inward and PNP formation was confirmed by using Scan Spectra of solutions, whereas, in the case of BPNPP, the flow was outward. In case of BPNPP the flow generated was due to the interaction of BPNPP with Surfactant. There was no significant catalysis observed in case of BPNPP. The flow generated here is due to the density difference between the compounds, which causes pumping to switch direction. The flow switching behaviour due to the binding of substrate to the surfactant will also add dimension in supramolecular chemistry. Since in micropumps, small amounts of fluids move, these micropumps can be used to fabricate microfluidic devices which can transport molecules to a specific location. Flow behaviour inside the cell can be understood through this.

NMR characterization of compounds

^{1}H NMR spectra of 1E

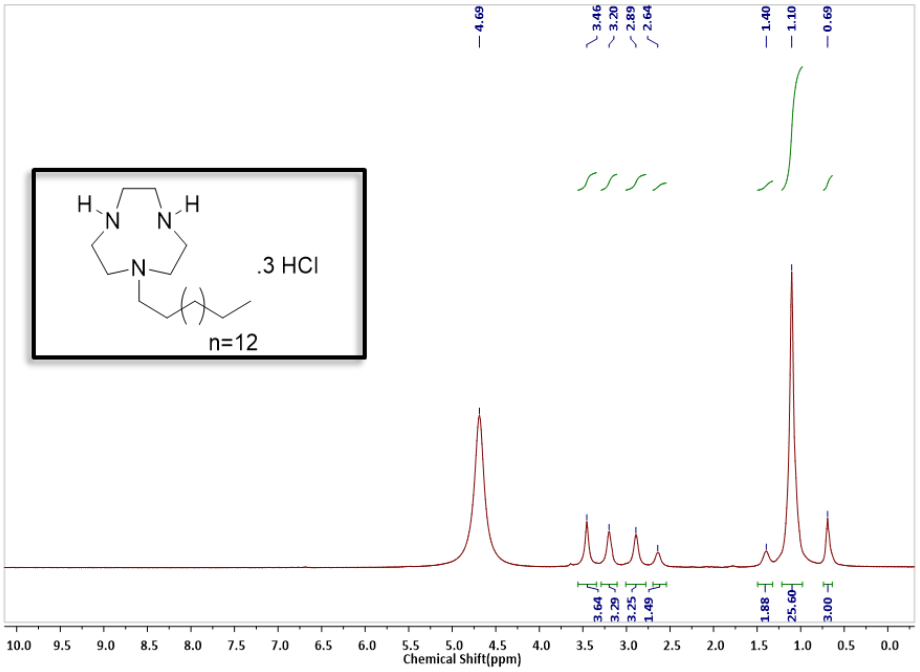

^{13}C NMR spectra of 1E

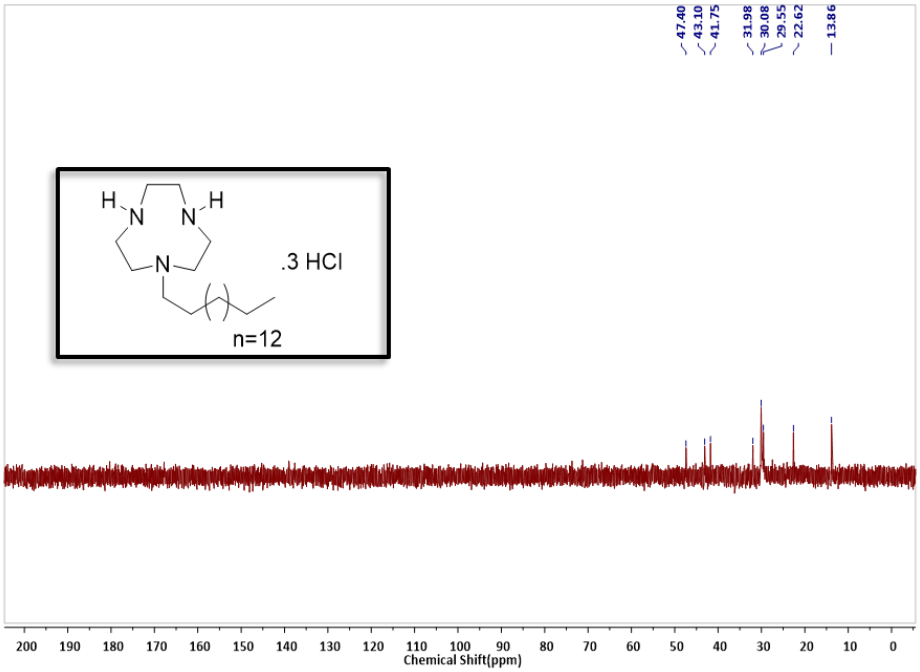

^{1}H NMR spectra of 2D

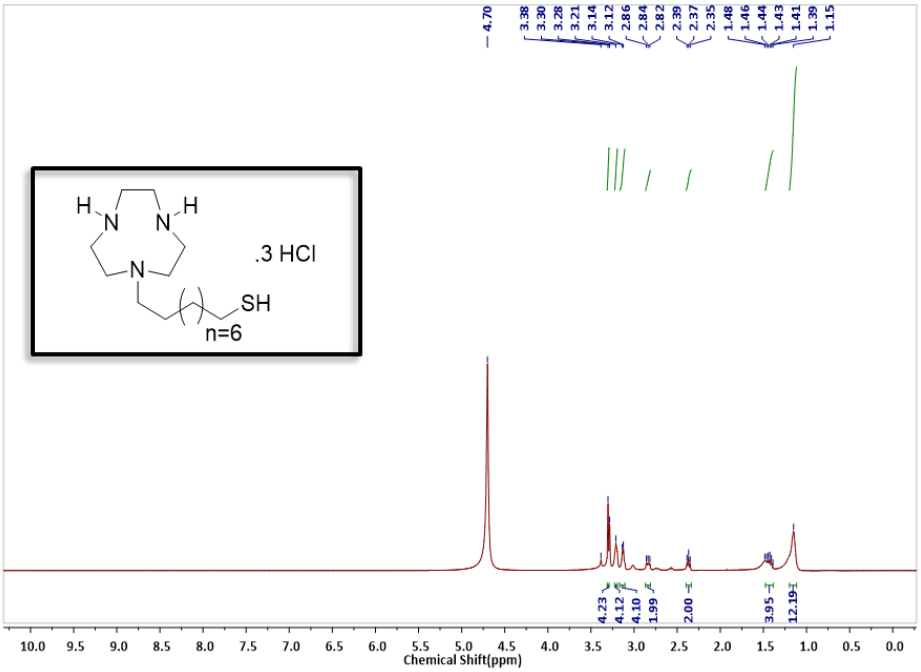

^{13}C NMR spectra of 2D

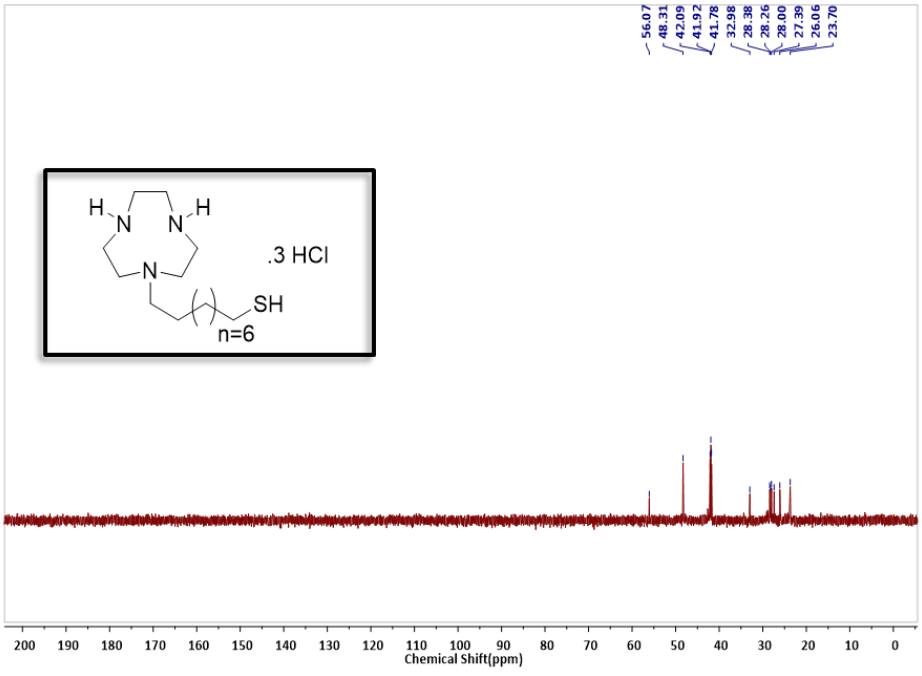

^{1}H NMR spectra of 3C

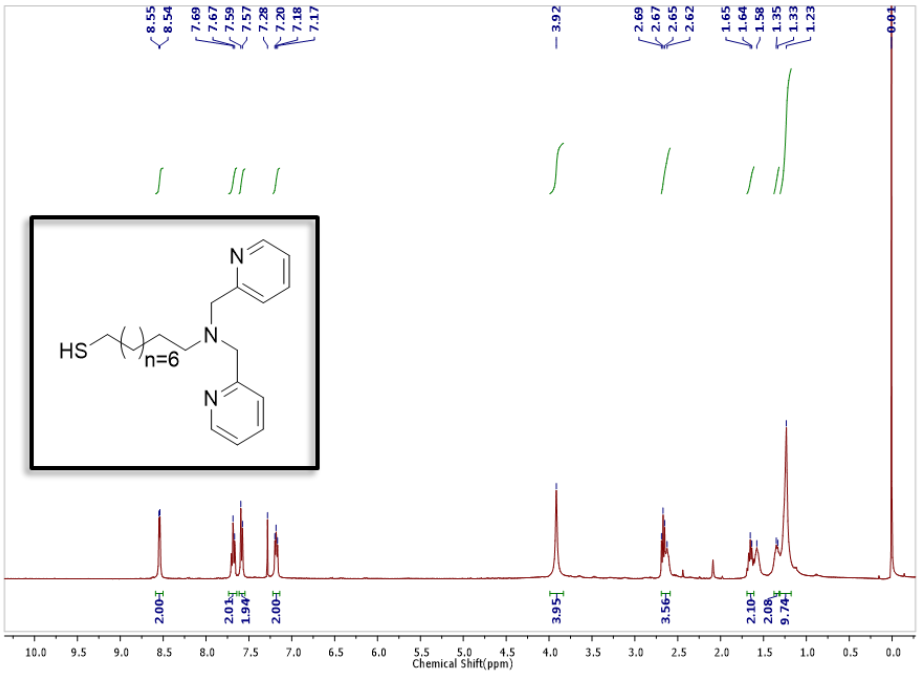

^{13}C NMR spectra of 3C

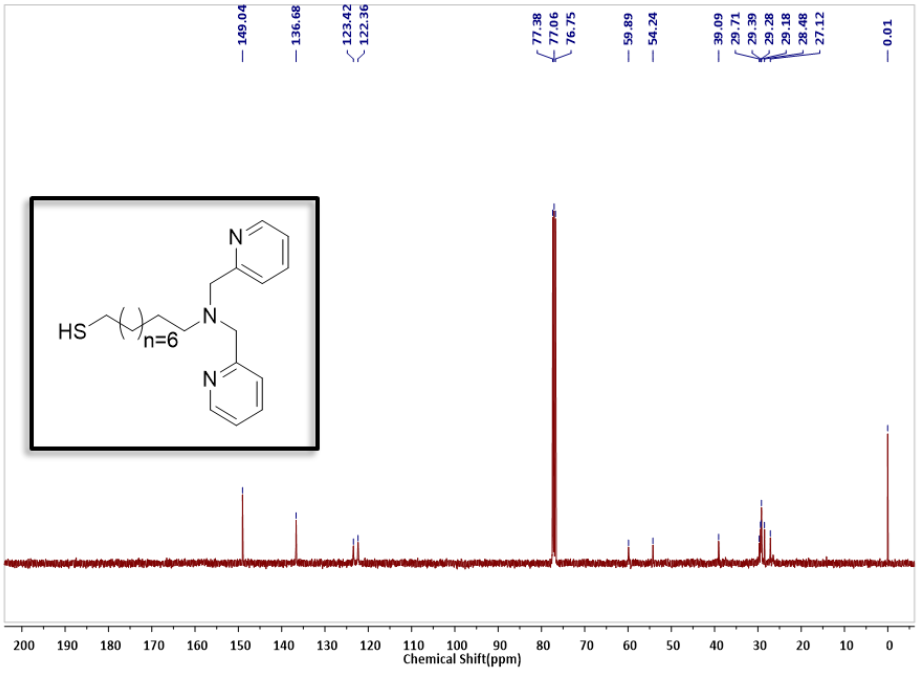

^{1}H NMR spectra of 4C

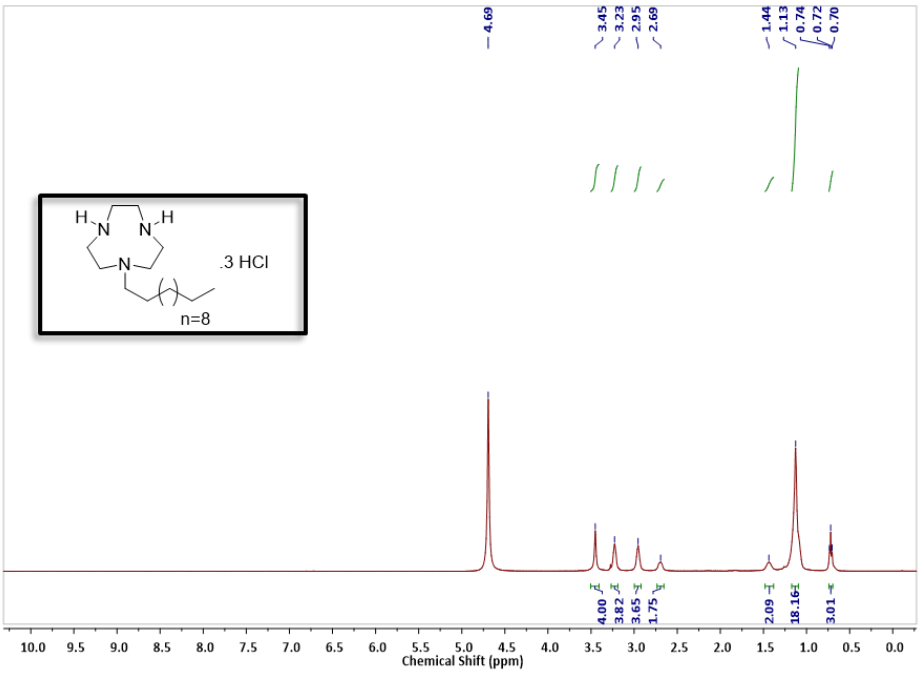

^{13}C NMR spectra of 4C

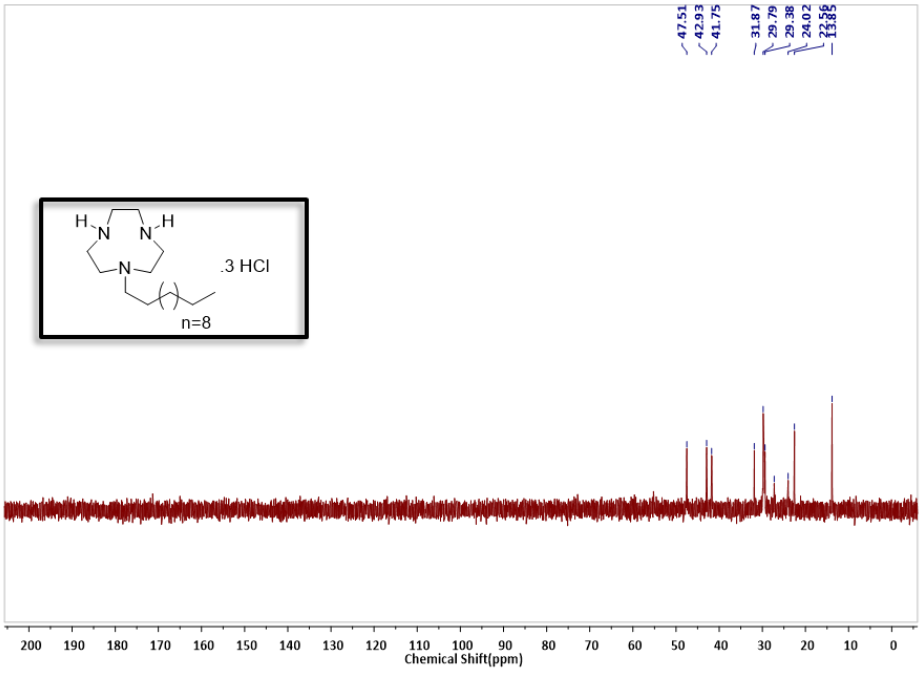

^{1}H NMR spectra of 5A

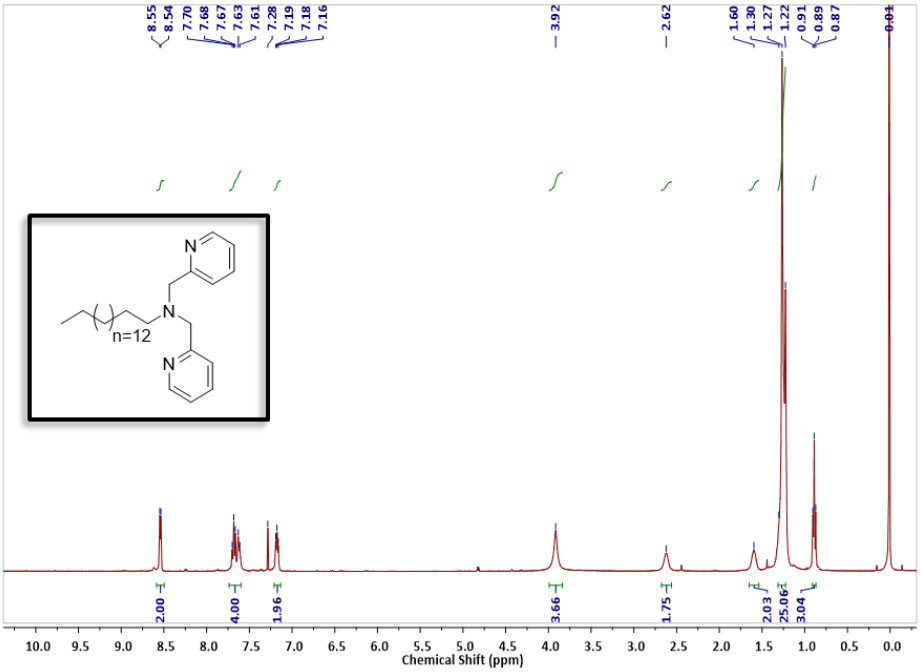

^{13}C NMR spectra of 5A

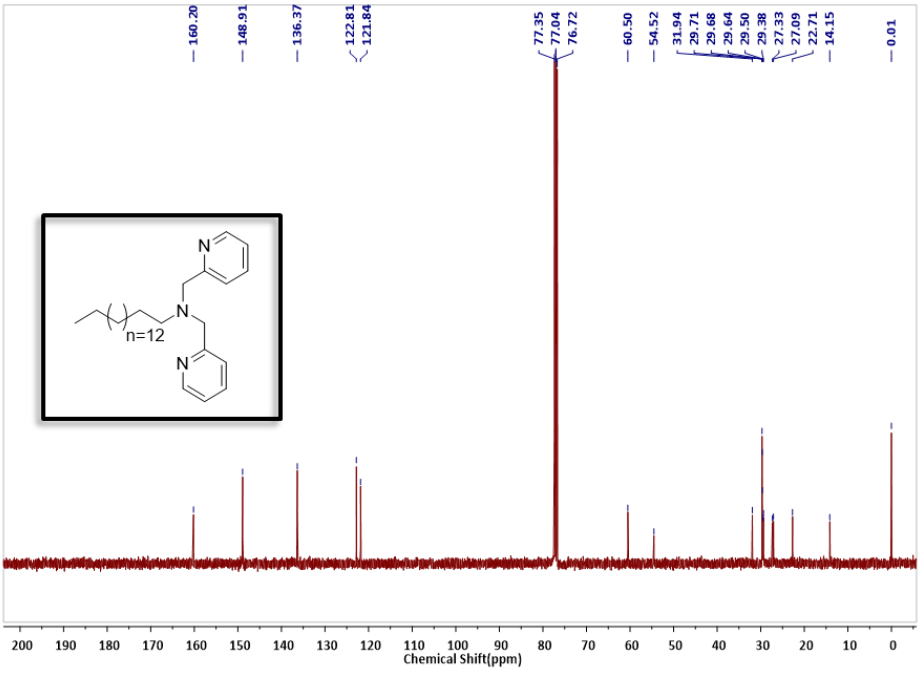

^{1}H NMR spectra of 6A

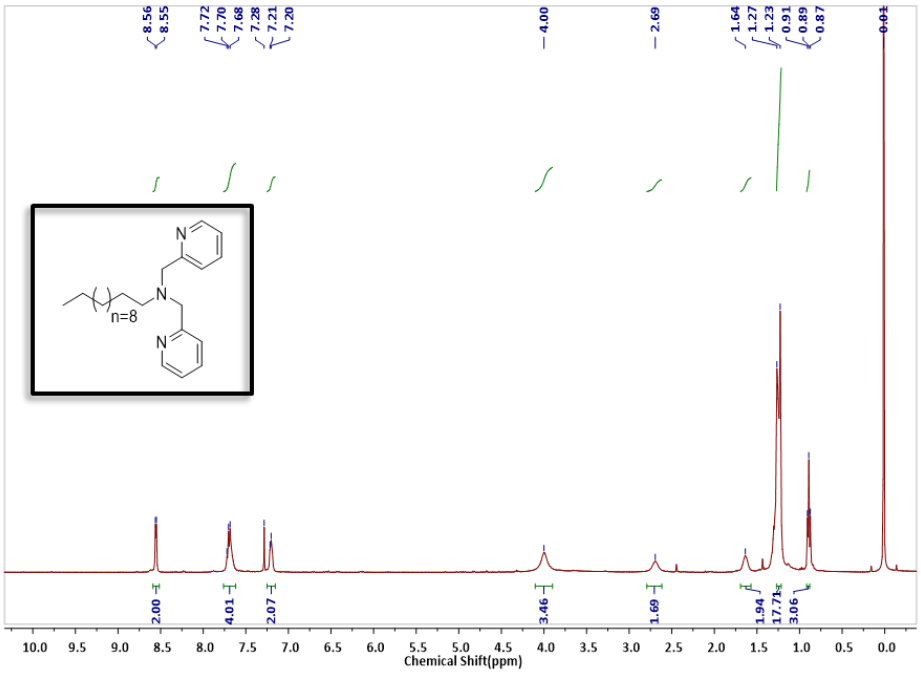

^{13}C NMR spectra of 6A

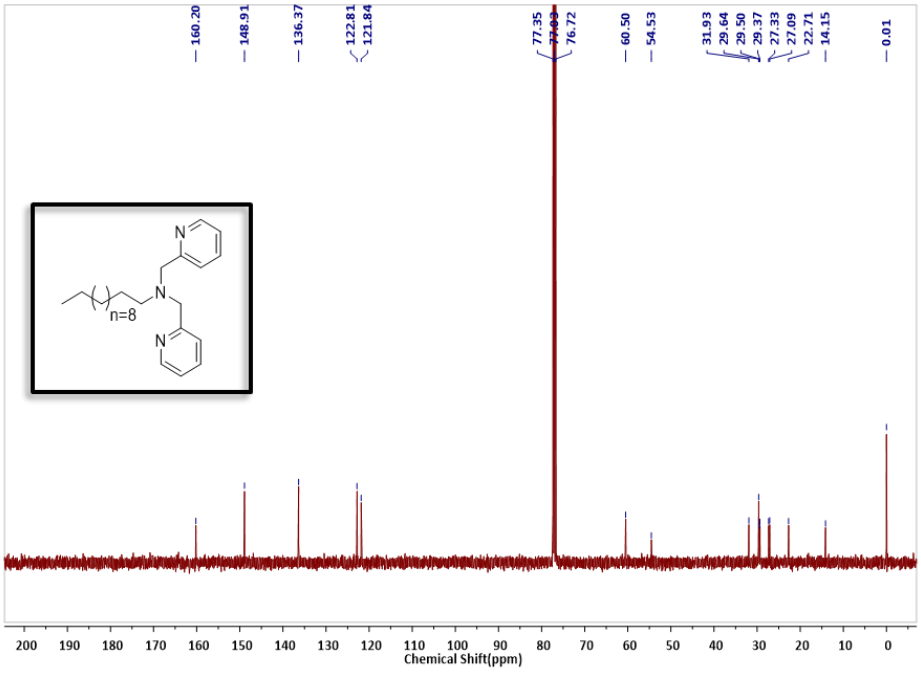

Bibliography

1. Durst, F. Introduction, Importance and Development of Fluid Mechanics. *Fluid Mech. An Introd. to Theory Fluid Flows* **2008**, 1–14.
2. Beebe, D. J.; Mensing, G. A.; Walker, G. M. Physics and Applications of Microfluidics in Biology. *Annu. Rev. Biomed. Eng.* **2002**, *4* (1), 261–286.
3. Whitesides, G. M. The Origins and the Future of Microfluidics. *Nature* **2006**, *442* (7101), 368–373.
4. https://www.news-medical.net/life-sciences/What-is-Microfluidics.aspx
5. Maillefer, D.; Gamper, S.; Frehner, B.; Balmer, P.; Lintel, H. V.; P. Renaud A high-performance silicon micropump for disposable drug delivery systems. 10.1109/MEMSYS.2001.906566Meeuwissen, J.; Reek, J. N. H. Supramolecular catalysis beyond enzyme mimics. *Nat. Chem.*, **2010,** *2*, 615-621.
6. Wheeler, A. R.; Throndset, W. R., Whelan, R. J., Leach, A. M.; Zare, R. N.; Liao, Y. H.; Farrell, K.; Manger, I. D.; Daridon, A. Microfluidic device for single-cell analysis. *Anal. Chem.* **2003**, *75*, 3581–3586.
7. Young, E. W. K.; Simmons, C. A. Macro-and Microscale Fluid Flow Systems for Endothelial Cell Biology. *Lab Chip* **2010**, *10* (2), 143–160.
8. https://en.wikipedia.org/wiki/Micropump
9. Sánchez, S.; Soler, L.; Katuri, J. Chemically Powered Micro- and Nanomotors. *Angew. Chemie Int. Ed.* **2015**, *54* (5), 1414–1444
10. Paxton, W. F.; Kistler, K. C.; Olmeda, C. C.; Sen, A.; Angelo, S. K. St.; Cao, Y.; Mallouk, T. E.; Lammert, P. E.; Crespi, V. H. Catalytic Nanomotors: Autonomous Movement of Striped Nanorods. *J. Am. Chem. Soc.* **2004**, 126, 13424–13431
11. Wang, W.; Chiang, T. Y.; Velegol, D.; Mallouk, T. E. Understanding the Efficiency of Autonomous Nano- and Microscale Motors. *J. Am. Chem. Soc.* **2013**, *135*, 10557–10565.
12. Kline, T. R.; Paxton, W. F.; Wang,Y.; Velegol, D.; Mallouk, T. E.; Sen, A. Catalytic Micropumps: Microscopic Convective Fluid Flow and Pattern Formation. *J. Am. Chem. Soc.* **2005**, 127, 17150–17151.

13. Sengupta, S.; Patra, D.; Rivera, I. O.; Agrawal, A.; Shklyaev, S.; Dey, K. K.; Figueroa, U. C.; Mallouk, T. E.; Sen, A. Self-powered enzyme micropumps. *Nat. Chem.* **2014**, *6*, 415–422.
14. Bürgi, T. Properties of the gold–sulphur interface: from self-assembled monolayers to clusters. ***Nanoscale***, **2015**, ***7***, 15553-15567
15. Gentile, K.; Maiti, S.; Brink, A.; Rallabandi, B.; Stone, H. A.; Sen, A. Silver-Based Self-Powered pH-Sensitive Pump and Sensor. *Langmuir* **2020**, *36*, 7948–7955
16. Mikkola, S.; Lönnberg, T.; Lönnberg, H. Phosphodiester Models for Cleavage of Nucleic Acids. *Beilstein J. Org. Chem.* **2018**, *14* (1), 803–837
17. https://www.atdbio.com/content/2/Molecular-weight-and-mass
18. Pieters, G.; Cazzolaro, A.; Bonomi, R.; Prins, L. J. Self-assembly and selective exchange of oligoanions on the surface of monolayer protected Au nanoparticles in water. ***Chem. Commun.*** **2012**, ***48***, 1916-1918.
19. Maiti, S.; Fortunati, I.; Ferrante, C.; Scrimin, P.; Prins, L. J. Dissipative self-assembly of vesicular nanoreactors. *Nat. Chem.* **2016**, *8*, 725–731.
20. Feng, R.; Xu, Y.; Zhao, H.; Duan, X.; Sun, S. A Novel Platform Self-Assembled from Squaraine-Embedded Zn (II) Complexes for Selective Monitoring of ATP and Its Level Fluctuation in Mitotic Cells. *Analyst* **2016**, *141* (11), 3219–3223
21. Muñana, P.,S.; Ragazzon, G.; Dupont, J.; Ren, C. Z. J.; Prins, L. J.; Chen, J. L. Y. Substrate-Induced Self-Assembly of Cooperative Catalysts. *Angew. Chem.* **2018**, *57*, 16469-16474.
22. Pezzato, C.; Scrimin, P.; Prins. L. J. Zn^{2+}-Regulated Self-Sorting and Mixing of Phosphates and Carboxylates on the Surface of Functionalized Gold Nanoparticles. *Angew. Chem.* **2014**, *126*, 2136-2141.
23. Bonomi, R.; Selvestrel, F.; Lombardo, V.; Sissi, C.; Polizzi, S., Mancin, F.; Tonellato, U.; Scrimin, P. Phosphate Diester and DNA Hydrolysis by a Multivalent, Nanoparticle-Based Catalyst. *J. Am. Chem. Soc.* **2008**, *130*, 15744–15745.
24. Pieters, G.; Prins, L. J. Catalytic Self-Assembled Monolayers on Gold Nanoparticles. *New J. Chem.* **2012**, *36* (10), 1931–1939
25. Li, M.; Zhou, H.; Shi, L.; Li, D. W.; Long, Y. T. Ion-selective gold–thiol film on integrated screen-printed electrodes for analysis of Cu(II) ions.

Analyst, **2014**, ***139***, 643-648

26. https://www.sigmaaldrich.com/technical-documents/protocols/materials-science/thioacetate-deprotection.html?gclid=Cj0KCQiAhP2BBhDdARIsAJEzXlEEzjxREgTYerM4CCL08hyERk7rZO3rIMC61O9rMZq9SftfzPHfjEYaAswgEALw_wcB